

Dual-Uncertainty Guided Policy Learning for Multimodal Reasoning

Rui Liu^{*1,2}, Dian Yu¹, Tong Zheng², Runpeng Dai³, Zongxia Li², Wenhao Yu¹,
 Zhenwen Liang¹, Linfeng Song¹, Haitao Mi¹, Pratap Tokekare², Dong Yu¹

¹Tencent AI Lab, Bellevue

²University of Maryland, College Park

³University of North Carolina, Chapel Hill

Abstract

Reinforcement learning with verifiable rewards (RLVR) has advanced reasoning capabilities in multimodal large language models. However, existing methods typically treat visual inputs as deterministic, overlooking the perceptual ambiguity inherent to the visual modality. Consequently, they fail to distinguish whether a model’s uncertainty stems from complex reasoning or ambiguous perception, preventing the targeted allocation of exploration or learning signals. To address this gap, we introduce DUPL, a dual-uncertainty guided policy learning approach for multimodal RLVR that quantifies and leverages both perceptual uncertainty (via symmetric KL divergence) and output uncertainty (via policy entropy) to guide policy updates. By establishing an uncertainty-driven feedback loop and employing a dynamic branch prioritization mechanism, DUPL recalibrates the policy advantage to focus learning on states with high perceptual or decisional ambiguity, enabling effective targeted exploration beyond passive data augmentation. Implemented on top of GRPO and evaluated on six multimodal mathematical and general-domain reasoning benchmarks, DUPL improves Qwen2.5-VL 3B and 7B models, achieving accuracy gains of up to 11.2% on visual math tasks and up to 7.1% on general-domain reasoning tasks, while consistently outperforming GRPO. These results demonstrate that dual-uncertainty guided policy learning is an effective and generalizable approach for multimodal RLVR.

1 Introduction

Reinforcement learning with verifiable rewards (RLVR) has substantially improved the reasoning abilities of large language models (LLMs) by optimizing against ground-truth answers (Luong et al., 2024; Lambert et al., 2024; Guo et al., 2025; Su

et al., 2025; Zheng et al., 2025a). However, this outcome-centric approach often suppresses trajectories with valid intermediate reasoning steps that conclude with incorrect final answers, restricting exploration and yielding brittle policies (Dai et al., 2025). While text-only strategies mitigate this via uncertainty-aware objectives (Cheng et al., 2025), diversity-promoting rewards (Li et al., 2025a), pass@k rewards (Chen et al., 2025b; Walder and Karkhanis, 2025), intermediate feedback (Setlur et al., 2024), and entropy regularization (Cheng et al., 2025; Zhang et al., 2025; Cui et al., 2025; Wang et al., 2025a), these mechanisms operate strictly within the text or action space. As the paradigm shifts to Multimodal Large Language Models (MLLMs) (Huang et al., 2025; Tan et al., 2025; Peng et al., 2025), where textual reasoning is coupled with complex visual inputs, effective exploration becomes fundamentally more challenging and remains largely underexplored.

Current multimodal RLVR approaches typically treat visual input as a fixed, deterministic condition. This overlooks the inherent ambiguity of the visual modality, where ambiguous objects or multiple valid interpretations may exist. While recent approaches (Liu et al., 2025b; Yao et al., 2025) attempt to improve robustness via visual noise injection during rollout collection, these methods primarily rely on passive data augmentation that leaves the learning objective unchanged, resulting in undirected exploration rather than targeted exploration toward states of genuine uncertainty. Similarly, while perception-aware optimization can improve visual grounding (Wang et al., 2025c), it lacks a mechanism to model or leverage uncertainty to guide policy exploration.

This reveals a fundamental limitation in current multimodal RLVR: exploration strategies are **blind to the source of uncertainty**. By failing to distinguish whether a model’s uncertainty stems from complex reasoning or ambiguous perception,

^{*}Work done during an internship at Tencent AI Lab, Bellevue, WA.

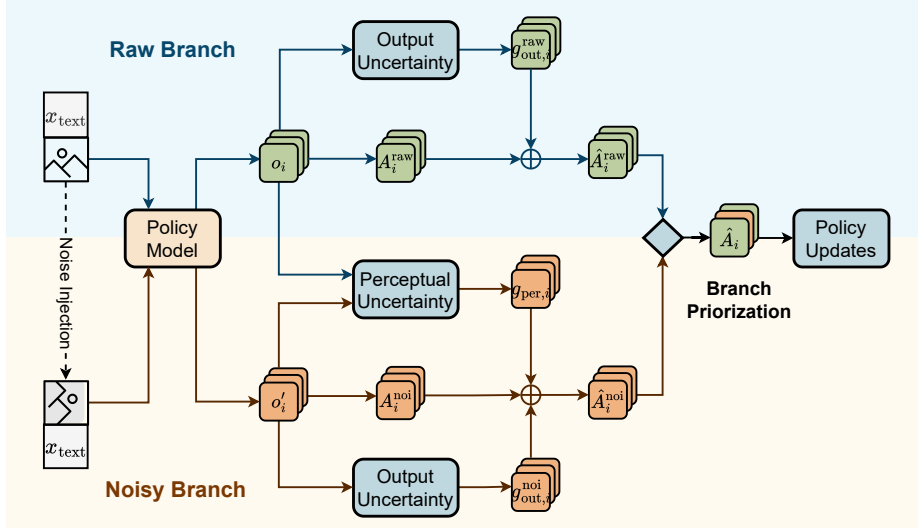


Figure 1: **Overview of DUPL for multimodal reasoning.** DUPL establishes a dual-uncertainty guided feedback loop for policy updates, capturing both perceptual and output uncertainty. The raw branch processes the original input, while the noisy branch processes a perturbed view. Perceptual uncertainty is quantified via token-level symmetric KL divergence between branches, producing the guidance signal g_{per} to shape the advantage. Output uncertainty is measured by policy entropy, generating guidance signals g_{out}^{raw} and g_{out}^{noi} for the raw and noisy branches, respectively. A dynamic branch prioritization mechanism emphasizes uncertainty-driven exploration early in training and gradually shifts focus to the raw branch as learning stabilizes.

existing methods cannot prioritize learning signals where they are most needed. Consequently, exploration remains inefficiently distributed. What is missing is a policy learning mechanism capable of **decoupling these uncertainty streams** to enable targeted, uncertainty-aware updates.

To address this gap, we introduce **DUPL**, a targeted exploration approach for multimodal RLVR through **Dual-Uncertainty** guided Policy Learning. Inspired by closed-loop control principles (Hjalmarsson, 2005), DUPL forms an uncertainty-driven feedback loop where model uncertainty serves as a measured feedback signal to actively regulate policy updates. Rather than encouraging exploration through indiscriminate, passive data augmentation (Liu et al., 2025b; Yao et al., 2025), DUPL explicitly explores where the model is uncertain, capturing both perceptual and output uncertainty. Specifically, we transform visual perturbations into an **active sensitivity probe**: for each training example, we perform a dual-branch forward pass on the original image and a perturbed view, quantifying **perceptual uncertainty** via the symmetric KL divergence between the induced policy distributions. In parallel, DUPL models **output uncertainty** via the policy’s entropy in the action space. By jointly leveraging these two uncertainties as guidance signals to shape advantage for policy updates, DUPL dy-

namically steers exploration toward perceptually and decision-wise ambiguous states. Furthermore, we employ a dynamic branch prioritization mechanism that emphasizes uncertainty-driven exploration early in training before shifting focus to the original view as learning stabilizes.

We implement DUPL on top of GRPO (Shao et al., 2024) and evaluate it on six multimodal reasoning benchmarks spanning mathematical and general domains: MathVerse (Zhang et al., 2024), MathVista (Lu et al., 2023), We-Math (Qiao et al., 2024), HallusionBench (Guan et al., 2024), ChartQA (Masry et al., 2022), and LogicVista (Xiao et al., 2024). Trained on the MMRL30k dataset (Zhu et al., 2025a), DUPL enhances Qwen2.5-VL models across both 3B and 7B scales (Bai et al., 2023). On visual mathematical reasoning tasks, DUPL achieves accuracy gains of up to 11.2% (Avg. 10.1%) for 3B and up to 7.9% (Avg. 7.1%) for 7B models, while on general-domain benchmarks it yields improvements of up to 7.1% (Avg. 6.0%) for 3B and up to 5.8% (Avg. 4.4%) for 7B models (Table 1 and Table 2). DUPL consistently outperforms GRPO, demonstrating the effectiveness of dual-uncertainty guided policy learning. In summary, the core contributions of our work are as follows:

- We identify a fundamental limitation in multimodal RLVR: the inability to distinguish be-

tween perceptual ambiguity and reasoning uncertainty, which leads to inefficient, undirected exploration.

- We introduce DUPL, a policy learning framework that decouples and quantifies perceptual and output uncertainty to recalibrate advantage through an uncertainty-driven feedback loop.
- We propose an active probing mechanism with dynamic branch prioritization, transforming visual perturbations from passive augmentation into a principled signal for targeted, uncertainty-aware optimization.
- Across six benchmarks, DUPL consistently outperforms GRPO baselines, achieving accuracy gains of up to 11.2% on visual math and 7.1% on general-domain reasoning tasks across both 3B and 7B scales.

2 Approach

We build upon Group Relative Policy Optimization (GRPO) (Shao et al., 2024) as the underlying RL algorithm in this work (see Appendix A.1 for preliminaries). Formally, given a multimodal input $x = (x_{\text{text}}, x_{\text{image}})$, we aim to optimize the MLLM policy network π_θ by maximizing a surrogate objective in Eq. 3 in Appendix A.1.

The core of our approach is to enable targeted exploration in multimodal RLVR through dual-uncertainty guided policy learning. Rather than relying on passive data augmentation, DUPL explicitly explores where the model is uncertain. To this end, we transform visual perturbations into an active sensitivity probe that quantifies perceptual uncertainty. In parallel, we quantify output uncertainty. These two uncertainties serve as active feedback signals: they are integrated into the advantage function to guide policy optimization, incentivizing the model to explore perceptually and decision-wise ambiguous states. Finally, a dynamic branch prioritization schedule modulates this process, steering the model to prioritize exploration in early stages before stabilizing on the raw view for convergence. The full procedure is summarized in Algorithm 1 in Appendix A.2.

Perceptual Uncertainty. Moving beyond the standard use of image augmentation for RL (Yarats et al., 2021; Laskin et al., 2020), we introduce controlled image perturbations and transform them into an active sensitivity probe that quantifies perceptual uncertainty by

measuring how the model’s output distribution varies under visual transformations. Variations in the model’s predictions reflect its sensitivity to plausible perturbations, and therefore identify states worthy of exploration.

Specifically, for each image x_{image} in the training dataset, we create a perturbed counterpart x'_{image} through a stochastic augmentation function \mathcal{T} . This function applies a composition of transformations: $x'_{\text{image}} = \mathcal{T}(x_{\text{image}})$, where \mathcal{T} includes random horizontal/vertical flips, rotations, color jittering, and the addition of Gaussian noise. Then we employ a dual-branch forward pass, as illustrated in Figure 1. The raw branch processes the original input $x = (x_{\text{text}}, x_{\text{image}})$ to produce an output probability distribution $p = \pi_\theta(\cdot|x)$, while the noisy branch uses the perturbed input $x' = (x_{\text{text}}, x'_{\text{image}})$ to produce a distribution $q = \pi_\theta(\cdot|x')$. After obtaining the two distributions, we represent the perceptual uncertainty u_{per} as the divergence between them. We measure it using a symmetric KL divergence, which is calculated as the mean of the forward and backward KL divergences, encouraging exploration while maintaining stability:

$$u_{\text{per}} = \frac{1}{2} (\text{D}_{\text{KL}}(p||q) + \text{D}_{\text{KL}}(q||p)). \quad (1)$$

Output Uncertainty. After modeling the perceptual uncertainty, to promote general policy stochasticity and exploration in the action space, we model the output uncertainty u_{out} , which is based on the token entropy of the policy’s output distribution: $u_{\text{out}} = -\sum_{v \in \mathcal{V}} \pi_\theta(v | x, o_{<t}) \log \pi_\theta(v | x, o_{<t})$, where \mathcal{V} denotes the vocabulary.

Dual-Uncertainty Guided Policy Learning. After obtaining the two uncertainties, we integrate them into the advantage function to guide policy learning. We maintain separate advantage calculations for the raw and noisy branches. For the raw branch, we compute the output guidance signal induced by the output uncertainty, which is defined as: $g_{\text{out}} = \min\left(\frac{|A|}{\beta_o}, \alpha_o \cdot \text{stopgrad}(u_{\text{out}})\right)$, where α_o and β_o are scaling factors, $\text{stopgrad}(\cdot)$ is the stop gradient operator, which modulates the update magnitude without affecting gradient propagation.

For the noisy branch, except the output guidance signal, a perceptual guidance signal is incorporated, derived from the measured percep-

tual uncertainty, which is defined as: $g_{\text{per}} = \min\left(\frac{|A^{\text{noi}}|}{\beta_p}, \alpha_p \cdot \text{stopgrad}(u_{\text{per}})\right)$, where A^{noi} is the advantage for the noisy branch, α_p and β_p are scaling factors.

Therefore, for the raw branch, the uncertainty-guided advantage is calculated as: $\hat{A}^{\text{raw}} = A^{\text{raw}} + g_{\text{out}}^{\text{raw}}$, and for the noisy branch: $\hat{A}^{\text{noi}} = A^{\text{noi}} + g_{\text{out}}^{\text{noi}} + g_{\text{per}}$. When implementing DUPL, we use GRPO’s standard estimator to compute the base advantages A^{noi} and A^{raw} (see Eq. 2 in Appendix A.1). Policy updates are then performed using the corresponding uncertainty-guided advantage, depending on the branch selected at each training step.

Dynamic Branch Prioritization. During training, it is crucial to balance the aggressive exploration driven by the noisy branch with the stable learning provided by the raw branch. A policy trained exclusively on the noisy branch may become overly stochastic and fail to converge, while a policy trained solely on the raw branch may not explore enough to find the optimal path. To manage this trade-off, we employ a dynamic branch prioritization strategy. At each training step, we stochastically choose which advantage estimate to use for the policy update. We define p_{noi} as the probability of prioritizing the noisy branch, which is expressed as: $p_{\text{noi}}(s) = \max(0, 1 - \frac{s}{s_{\text{total}}})$, where s is the current training step, s_{total} is the total training steps. This probability is decayed over the course of training. Initially, p_{noi} is high to promote broad exploration of the state space. As training progresses, p_{noi} is gradually decreased, causing the optimizer to favor the more stable advantage estimates from the raw branch.

3 Experiments

3.1 Experimental Setup

Implementation Details. We conduct direct RL training on top of Qwen2.5-VL-3B and 7B (Bai et al., 2023) models. The models are trained to generate responses in a structured format, where the reasoning process is enclosed within `<think></think>` tags and the final answer is presented in `\boxed{}`. We train all models on the MMRL30k dataset (Zhu et al., 2025a), which contains around 30K samples. The implementation builds on the framework EasyR1 (Zheng et al., 2025b).

To inject perturbation into images, we apply random horizontal/vertical flips, rotations, color jittering, and the addition of Gaussian noise with

zero mean and standard deviation $\sigma = 0.4$. A sensitivity analysis on different noise levels is provided in Section 3.4. We adopt a global batch size of 128, a rollout batch size of 256, and generate 5 rollouts per input. For more training details, please see Appendix A.4.

Evaluation. We evaluate accuracy on six multimodal reasoning benchmarks for model generalization performance, including MathVerse (Zhang et al., 2024), MathVista (Lu et al., 2023), WeMath (Qiao et al., 2024), HallusionBench (Guan et al., 2024), ChartQA (Masry et al., 2022), and LogicVista (Xiao et al., 2024). These benchmarks span diverse aspects of multimodal reasoning, covering mathematical problem solving, hallucination detection, chart understanding, and logical reasoning. We follow the evaluation protocol of Zhu et al. (2025a) and use Qwen2.5-72B-Instruct (Team, 2024) to extract final answers from model responses and assess their correctness against reference answers.

We compare DUPL with the Qwen2.5-VL 3B and 7B base models, as well as the strong baseline GRPO (Shao et al., 2024). For broader context, we also report evaluated results from prior 7B models: R1-Onevision-7B (Yang et al., 2025), OpenVLThinker-7B (Deng et al., 2025), VLAA-Thinker-7B (Chen et al., 2025a), MM-Eureka-Qwen-7B (Meng et al., 2025), ThinkLite-VL-7B (Wang et al., 2025b), and NoisyRollout (Liu et al., 2025b).

3.2 Main Results

We first evaluate DUPL on multimodal mathematical reasoning benchmarks, including MathVerse, MathVista, and WeMath (Table 1). Compared to the Qwen2.5-VL base models, DUPL improves accuracy by up to 11.2% (Avg. 10.1%) for the 3B model and up to 7.9% (Avg. 7.1%) for the 7B model. DUPL also consistently outperforms the strong RLVR baseline GRPO across all benchmarks, indicating more effective policy learning for multimodal mathematical reasoning.

To assess generalization beyond mathematical reasoning, we further evaluate DUPL on general-domain reasoning benchmarks, including HallusionBench, ChartQA, and LogicVista (Table 2). Compared to the base models, DUPL achieves gains of up to 7.1% (Avg. 6.8%) for the 3B model and up to 5.8% (Avg. 4.4%) for the 7B model, again outperforming GRPO on all tasks. Notably, DUPL-7B attains the best average performance

Model	MathVerse	MathVista	WeMath	Avg.
SFT + RL				
R1-Onevision-7B (Yang et al., 2025)	46.0	63.9	61.8	57.2
OpenVLThinker-7B (Deng et al., 2025)	48.0	70.0	67.1	61.7
VLAA-Thinker-7B (Chen et al., 2025a)	48.2	68.3	67.7	61.4
Zero RL				
MM-Eureka-Qwen-7B (Meng et al., 2025)	50.3	71.2	65.6	62.4
ThinkLite-VL-7B (Wang et al., 2025b)	47.3	71.9	69.2	52.8
NoisyRollout-7B (Liu et al., 2025b)	51.0	72.6	70.3	64.6
Qwen2.5-VL-3B (Bai et al., 2023)	34.0	58.4	51.8	48.1
GRPO-3B	40.6	66.4	60.8	55.9
DUPL-3B (Ours)	42.7	68.9	63.0	58.2
Qwen2.5-VL-7B (Bai et al., 2023)	45.8	67.2	63.2	58.7
GRPO-7B	48.0	70.6	68.5	62.4
VOGUE-7B (Ours)	52.1	74.2	71.1	65.8

Table 1: **Model accuracy on diverse visual mathematical reasoning benchmarks.** We compare DUPL against GRPO and Qwen2.5-VL base models, and also report results from prior SFT+RL and Zero-RL methods following the evaluation protocol of Zhu et al. (2025a). Relative to the Qwen2.5-VL base models, DUPL achieves gains of up to **11.2%** (Avg. 10.1%) for the 3B model and **7.9%** (Avg. 7.1%) for the 7B model. DUPL also consistently outperforms GRPO, with DUPL-7B achieving the strongest average performance across all benchmarks.

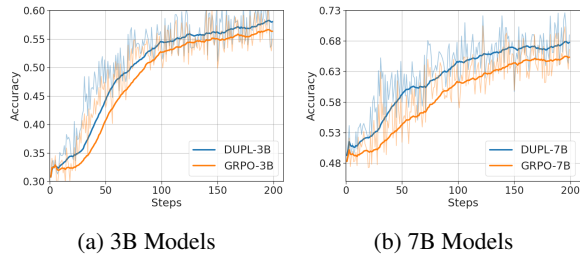


Figure 2: **Training accuracy rewards of DUPL and GRPO on Qwen2.5-VL 3B and 7B models.** DUPL consistently achieves higher rewards than GRPO throughout training.

across these benchmarks. Consistent with these results, the training accuracy reward curves in Figure 2 show that DUPL maintains higher rewards than GRPO throughout training for both model scales, suggesting more effective policy learning.

Taken together, these results demonstrate that DUPL yields consistent and robust improvements across both mathematical and general-domain multimodal reasoning tasks. The observed gains support our hypothesis that explicitly guiding exploration with perceptual and output uncertainty enables more effective policy updates, rather than relying on passive data augmentation or undirected exploration.

3.3 Ablation Studies

To validate the contribution of each component in DUPL, including perceptual uncertainty, output

uncertainty, dynamic branch prioritization strategy, as well as the influence of alternative divergence measures. We perform a series of ablation studies using the Qwen2.5-VL-7B model.

Perceptual Uncertainty. We first investigate the specific contribution of perceptual uncertainty by performing an ablation study where the term u_{per} is deactivated. We report the quantitative results for visual mathematical reasoning and general-domain benchmarks in Table 3 and Table 4, respectively. As shown, removing perceptual uncertainty from the feedback guidance results in an accuracy drop of up to 3.8% (Avg. 1.7%) on mathematical reasoning benchmarks. On general-domain reasoning tasks, performance decreases by up to 1.3% (Avg. 1.0%). We further illustrate the training dynamics in Figure 5 (see Appendix A.5). Without perceptual uncertainty, the learning curve consistently lags behind that of the full DUPL approach, indicating slower and less effective policy optimization. These results confirm that incorporating perceptual uncertainty as a feedback signal plays a critical role in guiding policy learning. By explicitly steering exploration toward visually uncertain states, perceptual uncertainty enables more targeted exploration, thereby improving the model’s reasoning accuracy.

Model	HallusionBench	ChartQA	LogicVista	Avg.
SFT + RL				
R1-Onevision-7B (Yang et al., 2025)	67.2	78.3	45.5	63.7
OpenVLThinker-7B (Deng et al., 2025)	60.0	78.9	47.1	62.0
VLAAThinker-7B (Chen et al., 2025a)	70.0	80.2	47.3	65.8
Zero RL				
MM-Eureka-Qwen-7B (Meng et al., 2025)	66.4	79.9	47.3	64.5
ThinkLite-VL-7B (Wang et al., 2025b)	70.9	81.4	48.9	67.1
NoisyRollout-7B (Liu et al., 2025b)	70.1	82.1	47.5	66.6
Qwen2.5-VL-3B (Bai et al., 2023)	59.9	73.1	38.0	57.0
GRPO-3B	65.5	77.6	39.3	60.8
DUPL-3B (Ours)	67.0	78.1	44.0	63.0
Qwen2.5-VL-7B (Bai et al., 2023)	65.2	79.8	45.5	63.5
GRPO-7B	68.6	81.9	46.0	65.5
VOGUE-7B (Ours)	71.0	84.0	48.7	67.9

Table 2: **Model accuracy on diverse visual general-domain reasoning benchmarks.** We compare DUPL against GRPO and Qwen2.5-VL base models, and also report results from prior SFT+RL and Zero-RL methods following the evaluation protocol of Zhu et al. (2025a). Relative to the Qwen2.5-VL base models, DUPL improves accuracy by up to **7.1%** (Avg. 6.0%) for the 3B model and **5.8%** (Avg. 4.4%) for the 7B model. DUPL also consistently outperforms GRPO, with DUPL-7B achieving the strongest average performance across all benchmarks.

Approach	MathVerse	MathVista	WeMath	Avg.
Full approach	52.1	74.2	71.1	65.8
w/o u_{per}	48.3	73.6	70.3	64.1
w/o u_{out}	48.6	73.5	70.8	64.3
w/o u_{per} & u_{out}	48.0	73.1	68.5	63.2

Table 3: **Ablations of DUPL accuracy on visual mathematical reasoning benchmarks.** Ablations show that removing perceptual uncertainty u_{per} or output uncertainty u_{out} reduces performance, with the largest drop when both are removed, confirming their complementary benefits.

Approach	HallusionBench	ChartQA	LogicVista	Avg.
Full approach	71.0	84.0	48.7	67.9
w/o u_{per}	69.7	83.4	47.8	66.9
w/o u_{out}	70.2	82.4	47.8	66.8
w/o u_{per} & u_{out}	69.2	82.1	46.4	65.9

Table 4: **Ablations of DUPL on visual general-domain reasoning benchmarks.** The same ablation trend observed in mathematical reasoning holds in general-domain settings, indicating that perceptual uncertainty and output uncertainty generalize beyond math tasks.

Output Uncertainty. Next, we evaluate the impact of output uncertainty by removing the term u_{out} . We report the results on visual mathematical reasoning benchmarks in Table 3, and the results on general-domain reasoning in Table 4. In the absence of output uncertainty guidance, accuracy drops by up to 3.5% (Avg. 1.5%) on mathematical benchmarks and by up to 1.6% (Avg. 1.1%) on general-domain tasks. As illustrated by the train-

ing accuracy curves in Figure 5 (Appendix A.5), the variant without output uncertainty lags behind compared to the full DUPL approach.

Furthermore, jointly removing both perceptual and output uncertainty results in a more pronounced performance degradation. As shown in Tables 3 and 4, this combined ablation leads to accuracy drops of up to 4.1% (Avg. 2.6%) on mathematical reasoning benchmarks and up to 2.3% (Avg. 2.0%) on general-domain reasoning tasks.

These results demonstrate that both uncertainties provide effective and complementary feedback signals for policy optimization. Perceptual uncertainty encourages targeted exploration within the visual state space, while output uncertainty induces beneficial stochasticity in the textual output space.

Alternative Divergence Measures. To ablate the formulation of perceptual uncertainty, we replace the symmetric KL divergence with a forward KL variant. However, as shown in the training dynamics in Figure 3a, the forward KL divergence leads to unstable training with accuracy declining. We qualitatively analyze the evolution of perceptual uncertainty under different KL formulations throughout training. As illustrated in Figure 3b, perceptual uncertainty measured by forward KL grows excessively large, whereas uncertainty computed using symmetric KL exhibits a moderate in-

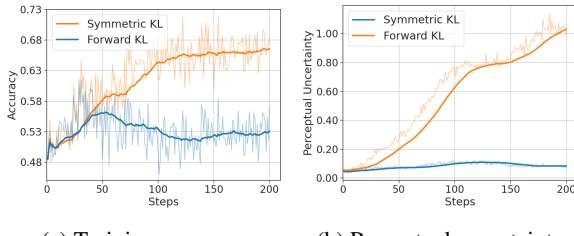


Figure 3: **Training accuracy and qualitative analysis of perceptual uncertainty under different divergence measures.** Measuring perceptual uncertainty with symmetric KL provides a stable signal that effectively guides policy learning while maintaining training stability. In contrast, forward KL produces excessively large perceptual uncertainty, resulting in unstable training and decreased accuracy.

crease followed by a gradual decrease, remaining overall stable during training. This observation explains the degraded performance under forward KL: it encourages the model to diverge excessively, leading to unstable policy updates. We also evaluate both variants on mathematical and general-domain reasoning benchmarks (Tables 5 and 6). Consistent with Figure 3, the forward KL formulation results in lower accuracy across all benchmarks.

Overall, this ablation validates the use of symmetric KL for measuring perceptual uncertainty, as it provides a stable uncertainty signal that supports effective exploration while preserving training stability.

Approach	MathVerse	MathVista	WeMath	Avg.
Forward KL	39.4	70.7	56.1	55.4
Symmetric KL	52.1	74.2	71.1	65.8

Table 5: **DUPL accuracy on mathematical reasoning benchmarks under different divergence measures.** Symmetric KL provides stable uncertainty guidance and improves accuracy, while forward KL induces excessive divergence and degrades performance.

Approach	HallusionBench	ChartQA	LogicVista	Avg.
Forward KL	67.5	80.3	45.1	64.3
Symmetric KL	71.0	84.0	48.7	67.9

Table 6: **DUPL accuracy on general-domain reasoning benchmarks under different divergence measures.** Symmetric KL enables stable uncertainty-guided learning, while forward KL leads to excessive divergence and degraded performance.

Dynamic Branch Prioritization. We evaluate the effect of the dynamic branch prioritization mechanism, which gradually adjusts the probability of selecting the noisy branch versus the raw

branch. To isolate its effect, we replace it with a fixed sampling probability of 0.5. We report the results on mathematical and general-domain reasoning benchmarks in Table 7 and Table 8, respectively. As shown, dynamic branch prioritization consistently outperforms fixed-probability sampling, yielding accuracy improvements of up to 3.6% (Avg. 2.5%) on mathematical reasoning benchmarks and up to 1.8% (Avg. 1.4%) on general-domain reasoning benchmarks. Similar trends are observed in the training curves shown in Figure 6 (Appendix A.5).

These results highlight the advantage of dynamic branch prioritization: higher reliance on the noisy branch facilitates exploration during early training, while progressively emphasizing the raw branch stabilizes optimization and improves convergence in later stages.

Approach	MathVerse	MathVista	WeMath	Avg.
Fixed Prob	48.5	73.6	67.8	63.3
Branch Prioritization	52.1	74.2	71.1	65.8

Table 7: **DUPL accuracy on mathematical reasoning benchmarks evaluating dynamic branch prioritization.** Dynamic branch prioritization outperforms fixed-probability sampling.

Approach	HallusionBench	ChartQA	LogicVista	Avg.
Fixed Prob	69.9	82.6	46.9	66.5
Branch Prioritization	71.0	84.0	48.7	67.9

Table 8: **DUPL accuracy on general-domain reasoning benchmarks evaluating dynamic branch prioritization.** Dynamic branch prioritization outperforms fixed-probability sampling.

3.4 Sensitivity Analysis

We conduct a sensitivity analysis of DUPL under varying levels of noise by adjusting the standard deviation of the Gaussian perturbation in the noisy branch ($\sigma \in \{0.2, 0.4, 0.8\}$). Accuracy results on mathematical and general-domain reasoning benchmarks are reported in Table 9 and Table 10, respectively. The results indicate that moderate noise ($\sigma = 0.4$) achieves the highest accuracy. Low noise ($\sigma = 0.2$) provides insufficient visual exploration, whereas high noise ($\sigma = 0.8$) introduces excessive variance. This trend is further supported by the training accuracy curves in Figure 4a, as well as the qualitative analysis of perceptual uncertainty evolution over training under different noise levels in Figure 4b.

4 Related Work

Exploration in Text-Based Reasoning. Recent work on text-only RLVR has begun to tackle pol-

Approach	MathVerse	MathVista	WeMath	Avg.
$\sigma = 0.2$	48.4	74.0	68.8	63.7
$\sigma = 0.4$	52.1	74.2	71.1	65.8
$\sigma = 0.8$	49.2	73.5	66.8	63.2

Table 9: **DUPL accuracy on mathematical reasoning benchmarks with different noise levels.** Moderate noise ($\sigma = 0.4$) yields the best accuracy.

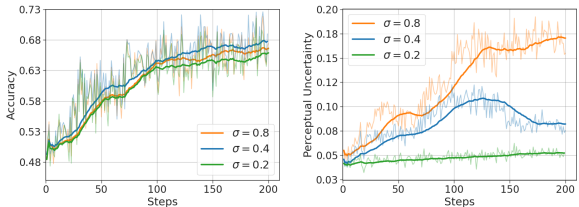
Approach	HallusionBench	ChartQA	LogicVista	Avg.
$\sigma = 0.2$	69.4	81.9	45.3	65.5
$\sigma = 0.4$	71.0	84.0	48.7	67.9
$\sigma = 0.8$	70.4	82.9	46.2	66.5

Table 10: **DUPL accuracy on general-domain reasoning benchmarks with different noise levels.** Moderate noise ($\sigma = 0.4$) yields the best accuracy.

icy exploration explicitly. Complementary to outcome rewards, i-MENTOR (Gao et al., 2025) incorporates trajectory-aware intrinsic signals and dynamic reward scaling to improve exploration for LLM reasoning. Replay-style methods, such as Retrospective Replay (Dou et al., 2025), revisit promising early states to prevent exploration decay later in training. Others have proposed outcome-based exploration schemes (Song et al., 2025) or have leveraged process rewards for more granular guidance (Setlur et al., 2024), though reliably scoring intermediate steps remains a challenge. Additionally, upweighting negative-sample reinforcement has been shown to mitigate diversity collapse and improve Pass@k (Zhu et al., 2025b), while EVOL-RL promotes reasoning diversity through novelty-oriented reinforcement without explicit labels (Zhou et al., 2025).

Multimodal RLVR. RLVR has been increasingly applied to enhance reasoning of multimodal models. Yang et al. (2025) extended language reasoning with visual inputs, improving visual question answering, while Huang et al. (2025) employed vision-grounded prompts to enhance multi-step reasoning. Deng et al. (2025) leveraged large-scale visual instruction tuning for improved cross-modal generalization, and Chen et al. (2025a) unified visual and textual signals in a policy-learning framework. Li et al. (2025b) proposed a self-rewarding approach that decomposes reasoning into visual perception and language reasoning. Wang et al. (2025c) added a perception-aware loss to improve visual grounding. Liu et al. (2025a) studied single-rollout RL to improve training efficiency for multimodal reasoning.

Despite these advances, effective exploration



(a) Training accuracy (b) Perceptual uncertainty

Figure 4: **Training accuracy and qualitative analysis of perceptual uncertainty under noise levels.** Moderate noise ($\sigma = 0.4$) yields the best performance.

during policy learning remains largely underexplored in multimodal RLVR. Most existing methods treat visual inputs as deterministic, overlooking perceptual ambiguity inherent to the visual modality. Recent work seeks to encourage exploration and improve visual robustness by injecting noise into training images (Liu et al., 2025b; Yao et al., 2025). However, these approaches rely on passive data augmentation, using noise to increase data diversity while leaving the policy learning objective unchanged. Consequently, exploration remains global and undirected, without targeting states characterized by genuine perceptual or decision uncertainty.

In contrast, DUPL introduces a targeted exploration approach for multimodal RLVR based on dual-uncertainty guided policy learning. By jointly modeling perceptual uncertainty and output uncertainty and incorporating them into an uncertainty-driven feedback loop, DUPL actively regulates policy updates and directs exploration toward states where the model is uncertain, addressing a key limitation of prior multimodal RLVR methods.

5 Conclusions

In conclusion, we introduce DUPL, a dual-uncertainty guided policy learning approach for multimodal RLVR. By measuring and leveraging both perceptual and output uncertainty, DUPL establishes an uncertainty-driven feedback loop that directs exploration toward states with genuine ambiguity, moving beyond passive data augmentation. Our approach integrates a dynamic branch prioritization mechanism and advantage shaping to effectively guide policy updates. Extensive experiments on six multimodal mathematical and general-domain reasoning benchmarks show that DUPL largely enhances the Qwen2.5-VL 3B and 7B models, achieving accuracy gains of up to 11.2% on visual math tasks and up to 7.1%

on general-domain reasoning tasks, while consistently outperforming strong baselines. These results demonstrate the effectiveness of targeted, uncertainty-guided policy learning.

Limitations

While DUPL effectively demonstrates the value of dual-uncertainty guided policy learning, our current implementation primarily relies on standard augmentation techniques, such as Gaussian noise and geometric manipulations, to induce perceptual uncertainty. A promising avenue for future investigation lies in exploring more sophisticated perturbation strategies or learnable noise generators that could expose subtler reasoning vulnerabilities. Furthermore, while we successfully unify perceptual and output uncertainty, our framework currently treats the textual input as fixed; extending this dual-uncertainty paradigm to incorporate textual input perturbations or adapting the methodology to dynamic modalities, such as video, presents a worthy direction for establishing a more comprehensive future work.

References

Jinze Bai, Shuai Bai, Shusheng Yang, Shijie Wang, Sinan Tan, Peng Wang, Junyang Lin, Chang Zhou, and Jingren Zhou. 2023. Qwen-vl: A versatile vision-language model for understanding, localization, text reading, and beyond. *arXiv preprint arXiv:2308.12966*.

Hardy Chen, Haoqin Tu, Fali Wang, Hui Liu, Xianfeng Tang, Xinya Du, Yuyin Zhou, and Cihang Xie. 2025a. Sft or rl? an early investigation into training rl-like reasoning large vision-language models. *arXiv preprint arXiv:2504.11468*.

Zhipeng Chen, Xiaobo Qin, Youbin Wu, Yue Ling, Qinghao Ye, Wayne Xin Zhao, and Guang Shi. 2025b. Pass@ k training for adaptively balancing exploration and exploitation of large reasoning models. *arXiv preprint arXiv:2508.10751*.

Daixuan Cheng, Shaohan Huang, Xuekai Zhu, Bo Dai, Wayne Xin Zhao, Zhenliang Zhang, and Furu Wei. 2025. Reasoning with exploration: An entropy perspective. *arXiv preprint arXiv:2506.14758*.

Ganqu Cui, Yuchen Zhang, Jiacheng Chen, Lifen Yuan, Zhi Wang, Yuxin Zuo, Haozhan Li, Yuchen Fan, Huayu Chen, Weize Chen, and 1 others. 2025. The entropy mechanism of reinforcement learning for reasoning language models. *arXiv preprint arXiv:2505.22617*.

Runpeng Dai, Linfeng Song, Haolin Liu, Zhenwen Liang, Dian Yu, Haitao Mi, Zhaopeng Tu, Rui Liu, Tong Zheng, Hongtu Zhu, and Dong Yu. 2025. Cde: Curiosity-driven exploration for efficient reinforcement learning in large language models. *Preprint, arXiv:2509.09675*.

Yihe Deng, Hritik Bansal, Fan Yin, Nanyun Peng, Wei Wang, and Kai-Wei Chang. 2025. Openvlthinker: Complex vision-language reasoning via iterative sft-rl cycles. *Preprint, arXiv:2503.17352*.

Shihan Dou, Muling Wu, Jingwen Xu, Rui Zheng, Tao Gui, Qi Zhang, and Xuanjing Huang. 2025. Improving rl exploration for llm reasoning through retrospective replay. *arXiv preprint arXiv:2504.14363*.

Jingtong Gao, Ling Pan, Yeting Wang, Rui Zhong, Chi Lu, Qingpeng Cai, Peng Jiang, and Xiangyu Zhao. 2025. Navigate the unknown: Enhancing llm reasoning with intrinsic motivation guided exploration. *arXiv preprint arXiv:2505.17621*.

Tianrui Guan, Fuxiao Liu, Xiyang Wu, Ruiqi Xian, Zongxia Li, Xiaoyu Liu, Xijun Wang, Lichang Chen, Furong Huang, Yaser Yacoob, and 1 others. 2024. Hallusionbench: an advanced diagnostic suite for entangled language hallucination and visual illusion in large vision-language models. In *Proceedings of the IEEE/CVF Conference on Computer Vision and Pattern Recognition*, pages 14375–14385.

Daya Guo, Dejian Yang, Haowei Zhang, Junxiao Song, Ruoyu Zhang, Runxin Xu, Qihao Zhu, Shirong Ma, Peiyi Wang, Xiao Bi, and 1 others. 2025. Deepseek-rl: Incentivizing reasoning capability in llms via reinforcement learning. *arXiv preprint arXiv:2501.12948*.

Håkan Hjalmarsson. 2005. From experiment design to closed-loop control. *Automatica*, 41(3):393–438.

Wenxuan Huang, Bohan Jia, Zijie Zhai, Shaosheng Cao, Zheyu Ye, Fei Zhao, Zhe Xu, Yao Hu, and Shaohui Lin. 2025. Vision-rl: Incentivizing reasoning capability in multimodal large language models. *arXiv preprint arXiv:2503.06749*.

Nathan Lambert, Jacob Morrison, Valentina Pyatkin, Shengyi Huang, Hamish Ivison, Faeze Brahman, Lester James V Miranda, Alisa Liu, Nouha Dziri, Shane Lyu, and 1 others. 2024. T\ ulu 3: Pushing frontiers in open language model post-training. *arXiv preprint arXiv:2411.15124*.

Misha Laskin, Kimin Lee, Adam Stooke, Lerrel Pinto, Pieter Abbeel, and Aravind Srinivas. 2020. Reinforcement learning with augmented data. *Advances in neural information processing systems*, 33:19884–19895.

Tianjian Li, Yiming Zhang, Ping Yu, Swarnadeep Saha, Daniel Khashabi, Jason Weston, Jack Lanchantin, and Tianlu Wang. 2025a. Jointly reinforcing diversity and quality in language model generations. *arXiv preprint arXiv:2509.02534*.

Zongxia Li, Wenhao Yu, Chengsong Huang, Rui Liu, Zhenwen Liang, Fuxiao Liu, Jingxi Che, Dian Yu, Jordan Boyd-Graber, Haitao Mi, and 1 others. 2025b. Self-rewarding vision-language model via reasoning decomposition. *arXiv preprint arXiv:2508.19652*.

Rui Liu, Dian Yu, Lei Ke, Haolin Liu, Yujun Zhou, Zhenwen Liang, Haitao Mi, Pratap Tokek, and Dong Yu. 2025a. Stable and efficient single-rollout rl for multimodal reasoning. *arXiv preprint arXiv:2512.18215*.

Xiangyan Liu, Jinjie Ni, Zijian Wu, Chao Du, Longxu Dou, Haonan Wang, Tianyu Pang, and Michael Qizhe Shieh. 2025b. Noisyrollout: Reinforcing visual reasoning with data augmentation. *arXiv preprint arXiv:2504.13055*.

Ilya Loshchilov and Frank Hutter. 2019. [Decoupled weight decay regularization](#). In *International Conference on Learning Representations*.

Pan Lu, Hritik Bansal, Tony Xia, Jiacheng Liu, Chunyu Li, Hannaneh Hajishirzi, Hao Cheng, Kai-Wei Chang, Michel Galley, and Jianfeng Gao. 2023. Mathvista: Evaluating mathematical reasoning of foundation models in visual contexts. *arXiv preprint arXiv:2310.02255*.

Trung Quoc Luong, Xinbo Zhang, Zhanming Jie, Peng Sun, Xiaoran Jin, and Hang Li. 2024. Reft: Reasoning with reinforced fine-tuning. *arXiv preprint arXiv:2401.08967*.

Ahmed Masry, Do Xuan Long, Jia Qing Tan, Shafiq Joty, and Enamul Hoque. 2022. Chartqa: A benchmark for question answering about charts with visual and logical reasoning. *arXiv preprint arXiv:2203.10244*.

Fanqing Meng, Lingxiao Du, Zongkai Liu, Zhixiang Zhou, Quanfeng Lu, Daocheng Fu, Tiancheng Han, Botian Shi, Wenhui Wang, Junjun He, and 1 others. 2025. Mm-eureka: Exploring the frontiers of multimodal reasoning with rule-based reinforcement learning. *arXiv preprint arXiv:2503.07365*.

Yingzhe Peng, Gongrui Zhang, Miaozen Zhang, Zhiyuan You, Jie Liu, Qipeng Zhu, Kai Yang, Xingzhong Xu, Xin Geng, and Xu Yang. 2025. Lmm-r1: Empowering 3b llms with strong reasoning abilities through two-stage rule-based rl. *arXiv preprint arXiv:2503.07536*.

Runqi Qiao, Qiuna Tan, Guanting Dong, Minhui Wu, Chong Sun, Xiaoshuai Song, Zhuoma GongQue, Shanglin Lei, Zhe Wei, MiaoXuan Zhang, and 1 others. 2024. We-math: Does your large multimodal model achieve human-like mathematical reasoning? *arXiv preprint arXiv:2407.01284*.

Amrith Setlur, Chirag Nagpal, Adam Fisch, Xinyang Geng, Jacob Eisenstein, Rishabh Agarwal, Alekh Agarwal, Jonathan Berant, and Aviral Kumar. 2024. Rewarding progress: Scaling automated process verifiers for llm reasoning. *arXiv preprint arXiv:2410.08146*.

Zhihong Shao, Peiyi Wang, Qihao Zhu, Runxin Xu, Junxiao Song, Xiao Bi, Haowei Zhang, Mingchuan Zhang, YK Li, Yang Wu, and 1 others. 2024. Deepseekmath: Pushing the limits of mathematical reasoning in open language models. *arXiv preprint arXiv:2402.03300*.

Yuda Song, Julia Kempe, and Remi Munos. 2025. Outcome-based exploration for llm reasoning. *arXiv preprint arXiv:2509.06941*.

Yi Su, Dian Yu, Linfeng Song, Juntao Li, Haitao Mi, Zhaopeng Tu, Min Zhang, and Dong Yu. 2025. Crossing the reward bridge: Expanding rl with verifiable rewards across diverse domains. *arXiv preprint arXiv:2503.23829*.

Huajie Tan, Yuheng Ji, Xiaoshuai Hao, Minglan Lin, Pengwei Wang, Zhongyuan Wang, and Shanghang Zhang. 2025. Reason-rft: Reinforcement fine-tuning for visual reasoning. *arXiv preprint arXiv:2503.20752*.

Qwen Team. 2024. [Qwen2.5: A party of foundation models](#).

Christian Walder and Deep Karkhanis. 2025. Pass@k policy optimization: Solving harder reinforcement learning problems. *arXiv preprint arXiv:2505.15201*.

Shenzhi Wang, Le Yu, Chang Gao, Chujie Zheng, Shixuan Liu, Rui Lu, Kai Dang, Xionghui Chen, Jianxin Yang, Zhenru Zhang, and 1 others. 2025a. Beyond the 80/20 rule: High-entropy minority tokens drive effective reinforcement learning for llm reasoning. *arXiv preprint arXiv:2506.01939*.

Xiyao Wang, Zhengyuan Yang, Chao Feng, Hongjin Lu, Linjie Li, Chung-Ching Lin, Kevin Lin, Furong Huang, and Lijuan Wang. 2025b. Sota with less: Mcts-guided sample selection for data-efficient visual reasoning self-improvement. *arXiv preprint arXiv:2504.07934*.

Zhenhailong Wang, Xuehang Guo, Sofia Stoica, Haiyang Xu, Hongru Wang, Hyeonjeong Ha, Xiusi Chen, Yangyi Chen, Ming Yan, Fei Huang, and 1 others. 2025c. Perception-aware policy optimization for multimodal reasoning. *arXiv preprint arXiv:2507.06448*.

Yijia Xiao, Edward Sun, Tianyu Liu, and Wei Wang. 2024. Logicvista: Multimodal llm logical reasoning benchmark in visual contexts. *arXiv preprint arXiv:2407.04973*.

Yi Yang, Xiaoxuan He, Hongkun Pan, Xiyan Jiang, Yan Deng, Xingtao Yang, Haoyu Lu, Dacheng Yin, Fengyun Rao, Minfeng Zhu, and 1 others. 2025. R1-onevision: Advancing generalized multimodal reasoning through cross-modal formalization. *arXiv preprint arXiv:2503.10615*.

Huanjin Yao, Qixiang Yin, Jingyi Zhang, Min Yang, Yibo Wang, Wenhao Wu, Fei Su, Li Shen, Minghui Qiu, Dacheng Tao, and 1 others. 2025. R1-sharevl: Incentivizing reasoning capability of multi-modal large language models via share-grpo. *arXiv preprint arXiv:2505.16673*.

Denis Yarats, Ilya Kostrikov, and Rob Fergus. 2021. Image augmentation is all you need: Regularizing deep reinforcement learning from pixels. In *International conference on learning representations*.

Jinghan Zhang, Xiting Wang, Fengran Mo, Yeyang Zhou, Wanfu Gao, and Kunpeng Liu. 2025. Entropy-based exploration conduction for multi-step reasoning. *arXiv preprint arXiv:2503.15848*.

Renrui Zhang, Dongzhi Jiang, Yichi Zhang, Haokun Lin, Ziyu Guo, Pengshuo Qiu, Aojun Zhou, Pan Lu, Kai-Wei Chang, Yu Qiao, and 1 others. 2024. Mathverse: Does your multi-modal llm truly see the diagrams in visual math problems? In *European Conference on Computer Vision*, pages 169–186. Springer.

Tong Zheng, Hongming Zhang, Wenhao Yu, Xiaoyang Wang, Xinyu Yang, Runpeng Dai, Rui Liu, Huiwen Bao, Chengsong Huang, Heng Huang, and 1 others. 2025a. Parallel-r1: Towards parallel thinking via reinforcement learning. *arXiv preprint arXiv:2509.07980*.

Yaowei Zheng, Junting Lu, Shenzhi Wang, Zhangchi Feng, Dongdong Kuang, and Yuwen Xiong. 2025b. Easyr1: An efficient, scalable, multi-modality rl training framework.

Yujun Zhou, Zhenwen Liang, Haolin Liu, Wenhao Yu, Kishan Panaganti, Linfeng Song, Dian Yu, Xiangliang Zhang, Haitao Mi, and Dong Yu. 2025. Evolving language models without labels: Majority drives selection, novelty promotes variation. *arXiv preprint arXiv:2509.15194*.

Linghao Zhu, Yiran Guan, Dingkang Liang, Jianzhong Ju, Zhenbo Luo, Bin Qin, Jian Luan, Yuliang Liu, and Xiang Bai. 2025a. Shuffle-r1: Efficient rl framework for multimodal large language models via data-centric dynamic shuffle. *arXiv preprint arXiv:2508.05612*.

Xinyu Zhu, Mengzhou Xia, Zhepei Wei, Wei-Lin Chen, Danqi Chen, and Yu Meng. 2025b. The surprising effectiveness of negative reinforcement in llm reasoning. *arXiv preprint arXiv:2506.01347*.

A Appendix

A.1 GRPO Preliminaries

We adopt GRPO (Shao et al., 2024) as the underlying RL algorithm in this work. In GRPO, given an input x , a group of responses $\{o_i\}_{i=1}^G$ are sampled from the old policy $\pi_{\theta_{\text{old}}}$, each associated with a reward r_i . Then the normalized advantage for response o_i is defined as:

$$A_i = \frac{r_i - \text{mean}(\{r_i\}_{i=1}^G)}{\text{std}(\{r_i\}_{i=1}^G)}. \quad (2)$$

As in PPO, GRPO uses clipped importance sampling to stabilize policy updates. Let $\rho_i(\theta) = \frac{\pi_\theta(o_i|x)}{\pi_{\theta_{\text{old}}}(o_i|x)}$ denote the probability ratio between the new and old policies. The GRPO objective is to maximize the following equation:

$$\mathcal{J}_{\text{GRPO}}(\theta) = \mathbb{E}_{x \sim \mathcal{D}, \{o_i\} \sim \pi_{\theta_{\text{old}}}} \left[\frac{1}{G} \sum_{i=1}^G \min \left(\rho_i(\theta) A_i, \text{clip}(\rho_i(\theta), 1 - \epsilon, 1 + \epsilon) A_i \right) \right], \quad (3)$$

where ϵ_{clip} is the clipping hyperparameter.

A.2 Algorithm

We present the full procedure of DUPL in Algorithm 1, summarizing Section 2. First, we measure output and perceptual uncertainty, which are then used to compute guidance signals. These signals are employed to shape the advantage for the raw and noisy branches separately. A dynamic branch prioritization mechanism is then applied to select which uncertainty-guided advantage is used for policy updates at each training step.

We express the policy gradient for the noisy branch as follows:

$$\nabla_\theta \mathcal{J}_{\text{DUPL}}(\theta) \propto \mathbb{E}_{o' \sim \pi_{\theta_{\text{old}}}} \left[(A^{\text{noi}} + g_{\text{out}}^{\text{noi}} + g_{\text{per}}) \cdot \nabla_\theta \log \pi_\theta(o' | x') \right]. \quad (4)$$

From a gradient perspective, this formulation encourages more effective policy updates for targeted exploration compared to standard RLVR approaches such as GRPO. We omit caps/clipping for clarity. The term $g_{\text{per}} \nabla_\theta \log \pi_\theta(o' | x')$ explicitly encourages the policy to increase the probability of action sequences that follow from perceptually uncertain states, guiding the model to acquire more informative visual features. There is also an

term g_{out} . This acts as a general-purpose exploration mechanism in the action space that complements the exploration driven by g_{per} . While g_{per} directs exploration toward perceptual uncertainty, g_{out} maintains stochasticity in the textual output space.

A.3 Prompt Templates

We list below the prompt used to instruct the model to produce the structured outputs.

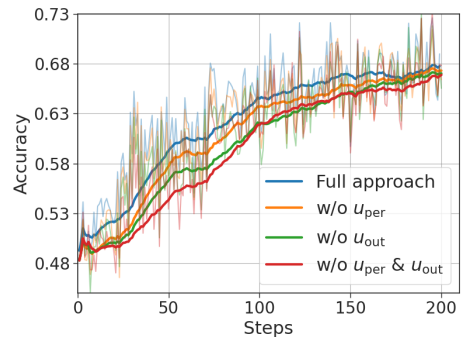
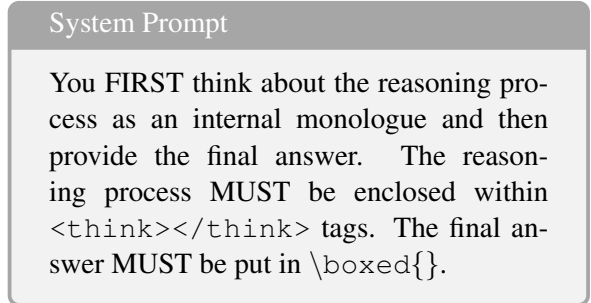


Figure 5: **Training dynamics of accuracy rewards under perceptual uncertainty u_{per} and output uncertainty u_{out} .** Each uncertainty signal provides effective feedback guidance and improves performance, while their combination of full approach yields the best results.

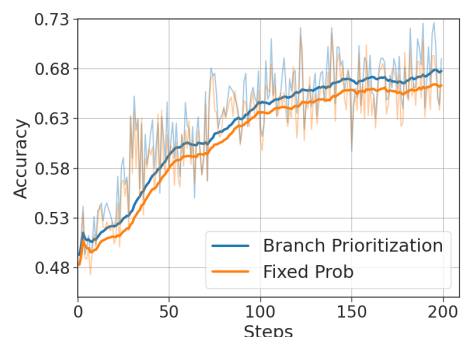


Figure 6: **Training dynamics of accuracy rewards comparing dynamic branch prioritization with fixed-probability sampling.** Dynamic branch prioritization consistently achieves higher accuracy.

Algorithm 1 Dual-Uncertainty Guided Policy Learning (DUPL)

Require: Dataset \mathcal{D} , group size G , total training steps s_{total} , augmentation function \mathcal{T} .

- 1: Initialize policy parameters θ , old policy $\theta_{\text{old}} \leftarrow \theta$
- 2: **for** $s = 1$ to s_{total} **do**
- 3: Sample input $x = (x_{\text{text}}, x_{\text{image}}) \sim \mathcal{D}$
- 4: Construct perturbed image $x'_{\text{image}} = \mathcal{T}(x_{\text{image}})$, $x' = (x_{\text{text}}, x'_{\text{image}})$
- 5: Sample group of responses $\{o_i\}_{i=1}^G \sim \pi_{\theta_{\text{old}}}(\cdot | x)$, $\{o'_i\}_{i=1}^G \sim \pi_{\theta_{\text{old}}}(\cdot | x')$
- 6: Compute branch prioritization probability: $p_{\text{noi}}(s) = \max(0, 1 - \frac{s}{s_{\text{total}}})$
- 7: **for** $i = 1$ to G **do**
- 8: Compute raw advantage A_i^{raw} , noisy advantage A_i^{noi} (Eq. 2)
- 9: Compute output uncertainty $u_{\text{out},i}^{\text{raw}}$ and $u_{\text{out},i}^{\text{noi}}$ for each branch
- 10: Compute perceptual uncertainty $u_{\text{per},i}$ using token-level symmetric KL divergence (Eq. 1)
- 11: Compute guidance signals:
$$g_{\text{per},i} = \min\left(\frac{|A_i^{\text{noi}}|}{\beta_p}, \alpha_p \cdot \text{stopgrad}(u_{\text{per},i})\right)$$

$$g_{\text{out},i}^{\text{raw}} = \min\left(\frac{|A_i^{\text{raw}}|}{\beta_o}, \alpha_o \cdot \text{stopgrad}(u_{\text{out},i}^{\text{raw}})\right), g_{\text{out},i}^{\text{noi}} = \min\left(\frac{|A_i^{\text{noi}}|}{\beta_o}, \alpha_o \cdot \text{stopgrad}(u_{\text{out},i}^{\text{noi}})\right)$$
- 12: Compute shaped advantages:
$$\hat{A}_i^{\text{raw}} = A_i^{\text{raw}} + g_{\text{out},i}^{\text{raw}}, \quad \hat{A}_i^{\text{noi}} = A_i^{\text{noi}} + g_{\text{out},i}^{\text{noi}} + g_{\text{per},i}$$
- 13: Sample branch selector $z_i \sim \text{Bernoulli}(p_{\text{noi}}(s))$
- 14: Select final advantage (with corresponding selected (x, o_i) or (x', o'_i)):
$$\hat{A}_i = z_i \cdot \hat{A}_i^{\text{noi}} + (1 - z_i) \cdot \hat{A}_i^{\text{raw}}$$
- 15: **end for**
- 16: Compute surrogate objective with shaped advantages (Eq. 3)
- 17: Update policy parameters $\theta \leftarrow \theta + \eta \nabla_{\theta} \mathcal{J}_{\text{DUPL}}(\theta)$
- 18: **end for**

A.4 Training Details

We train all models on the MMRL30k dataset (Zhu et al., 2025a), which contains around 30K samples. The models are trained to generate responses in a structured format, where the reasoning process is enclosed within `<think>/</think>` tags and the final answer is presented in `\boxed{}`. The reward function for RL training is a weighted combination of a format reward and an accuracy reward, with coefficients of 0.1 and 0.9, respectively. The training is performed for 200 steps using the AdamW optimizer (Loshchilov and Hutter, 2019) with a learning rate of $1e-6$ and a weight decay of 0.01. We adopt a global batch size of 128, a rollout batch size of 256, and generate 5 rollouts per input with a rollout temperature 1.0. The implementation builds on the framework EasyR1 (Zheng et al., 2025b).

When transferring perceptual and output uncer-

tainty into guidance signals for advantage shaping to guide policy learning, we use $\alpha_p = 1.0$ and $\beta_p = 2.0$ for perceptual uncertainty, and $\alpha_o = 0.4$ and $\beta_o = 2.0$ for output uncertainty, following the setup of Cheng et al. (2025).

A.5 Ablation Studies

In Section 3.3, we conduct a comprehensive set of ablation studies to validate the contribution of each component in DUPL, including perceptual uncertainty, output uncertainty, the dynamic branch prioritization strategy, and the choice of divergence measures. Here, we present additional results that further validate the role of some components.

In Figure 5, we show the training dynamics of accuracy rewards under perceptual uncertainty u_{per} and output uncertainty u_{out} . Each uncertainty signal provides effective feedback guidance and improves performance, while their combination in the full approach yields the best results.

We present the training dynamics of accuracy rewards in Figure 6, comparing dynamic branch prioritization with fixed-probability sampling. We observe that dynamic branch prioritization consistently achieves higher accuracy throughout training. These results highlight its advantage in balancing exploration and stability: increased reliance on the noisy branch facilitates exploration during early training, while progressively emphasizing the raw branch stabilizes optimization and improves convergence in later stages, leading to superior final performance.